Molecular Biology of the Cell
Vol. 10, 1163–1178, April 1999

Dynamics of a Chemoattractant Receptor in Living Neutrophils during Chemotaxis[V]

Guy Servant,* Orion D. Weiner,*† Enid R. Neptune,* John W. Sedat,† and Henry R. Bourne*‡

*Departments of Cellular and Molecular Pharmacology and of †Biochemistry and Biophysics, University of California San Francisco, San Francisco, California 94143

Submitted October 29, 1998; Accepted February 2, 1999
Monitoring Editor: J. Richard McIntosh

Persistent directional movement of neutrophils in shallow chemotactic gradients raises the possibility that cells can increase their sensitivity to the chemotactic signal at the front, relative to the back. Redistribution of chemoattractant receptors to the anterior pole of a polarized neutrophil could impose asymmetric sensitivity by increasing the relative strength of detected signals at the cell's leading edge. Previous experiments have produced contradictory observations with respect to receptor location in moving neutrophils. To visualize a chemoattractant receptor directly during chemotaxis, we expressed a green fluorescent protein (GFP)-tagged receptor for a complement component, C5a, in a leukemia cell line, PLB-985. Differentiated PLB-985 cells, like neutrophils, adhere, spread, and polarize in response to a uniform concentration of chemoattractant, and orient and crawl toward a micropipette containing chemoattractant. Recorded in living cells, fluorescence of the tagged receptor, C5aR–GFP, shows no apparent increase anywhere on the plasma membrane of polarized and moving cells, even at the leading edge. During chemotaxis, however, some cells do exhibit increased amounts of highly folded plasma membrane at the leading edge, as detected by a fluorescent probe for membrane lipids; this is accompanied by an apparent increase of C5aR–GFP fluorescence, which is directly proportional to the accumulation of plasma membrane. Thus neutrophils do not actively concentrate chemoattractant receptors at the leading edge during chemotaxis, although asymmetrical distribution of membrane may enrich receptor number, relative to adjacent cytoplasmic volume, at the anterior pole of some polarized cells. This enrichment could help to maintain persistent migration in a shallow gradient of chemoattractant.

INTRODUCTION

Chemotaxis, or directed cell movement up a chemical gradient, plays a central role in the accumulation of leukocytes at sites of infection and inflammation (Baggiolini, 1998). This motility is thought to depend on many cellular functions, including 1) protrusion and adhesion of the front end, driven by actin assembly; 2) contraction, probably driven by myosin-based motors, which moves nucleus and bulk cytoplasm in a forward direction; and 3) deadhesion of the trailing edge, thought to be partly mediated by the Ca^{2+}-sensitive enzymes, calcineurin and calpain (Cassimeris and Zigmond, 1990; Downey, 1994; Huttenlocher *et al.*, 1997). These processes are initiated in a coordinated manner by activation of chemoattractant receptors, members of the G protein-coupled receptor superfamily, located at the cell surface.

Neutrophilic leukocytes (neutrophils) can crawl up a chemotactic gradient that corresponds to a difference in chemoattractant concentration as low as 1% across the length of the cell (Zigmond, 1977), indicating that these cells can compare and efficiently amplify small differences in concentrations of the extracellular stim-

[V] Online version of this article contains video material for Figures 1, 2, 4, and 5. Online version available at www.molbiolcell.org.

‡ Corresponding author. E-mail address: h__bourne@quickmail.ucsf. edu.

ulus. Moreover, in a homogeneous solution or in a shallow gradient of chemoattractant, locomoting neutrophils tend to move persistently in a given direction, turning only at small angles (Zigmond, 1977; Zigmond *et al.*, 1981). Higher density of chemoattractant receptors at the leading edge of a polarized neutrophil could account for the asymmetrically distributed sensitivity underlying the ability to respond to a shallow gradient (Zigmond *et al.*, 1981). Such an asymmetric distribution of receptors would enhance the intensity of signal detected at the anterior pole of a moving neutrophil, relative to the rest of its surface. By steepening the apparent chemotactic gradient across the cell, asymmetrically distributed receptors would reinforce the cell's polarity and persistent forward motion (Zigmond, 1977; Zigmond *et al.*, 1981).

The lack of methods for direct observation of cell-surface proteins on living, moving neutrophils has led most investigators to rely on approaches that localize chemoattractant receptors on cells fixed after random polarization in a uniform concentration of chemoattractant. Such approaches, including the use of labeled ligands (Sullivan, *et al.*, 1984; Walter and Marasco, 1984, 1987) or anti-receptor antibodies (Gray, *et al.*, 1997), have led investigators to conclude that chemoattractant receptors are concentrated at the front (Walter and Marasco, 1984) or midregion (Sullivan, *et al.*, 1984) or are uniformly dispersed over the neutrophil surface (Walter and Marasco, 1987; Gray *et al.*, 1997). These discrepancies reflect different techniques and experimental conditions for localizing receptors, but might also result from fixing the cells at different times after application of the stimulus (Sullivan *et al.*, 1984; Walter and Marasco, 1984). The latter possibility would suggest that receptors may be distributed differently in different stages of the neutrophil response. Two groups have reported greater amounts of fluorescently labeled *N*-formyl-Met-Leu-Phe (fMLP),[1] a chemoattractant ligand, at the front of living polarized neutrophils, suggesting enrichment of the fMLP receptor at the leading edge (Schmitt and Bultmann, 1990; McKay *et al.*, 1991). These reports (Schmitt and Bultmann, 1990; McKay, *et al.*, 1991) did not indicate whether the increased fluorescence resulted from an increased concentration of receptor molecules per unit area of plasma membrane or from the increased folding of membranes that is seen (Davis, *et al.*, 1982; Cassimeris and Zigmond, 1990) at the leading edge of motile neutrophils.

[1] Abbreviations used: C5aR, C5a receptor; ChaCha, *N*-Met-Phe-Lys-ProdCha-Cha-dArg; CRAC, cytosolic regulator of adenylyl cyclase; DiD, 1,1′-dioctadecyl-3,3,3′,3′-tetramethylindodicarbocyanine perchlorate; FACS, fluorescence-activated cell sorting; fMLP, *N*-formyl-Met-Leu-Phe; GFP, green fluorescent protein; mHBSS, modified HBSS.

To observe receptors directly and in real time during chemotaxis, we sought to express in neutrophils a receptor linked to a fluorescent tag, green fluorescent protein (GFP). Neutrophils, however, are terminally differentiated, short lived in vitro, and refractory to most methods of transfection. Accordingly, we elected to use a cultured myeloid leukemia cell line, PLB-985, which can be induced by treatment with DMSO to differentiate into cells that display histochemical, morphological, and biochemical features of neutrophils (Tucker *et al.*, 1987; Dana *et al.*, 1998). Here we show that on a glass coverslip these cells also behave strikingly like neutrophils, adhering, spreading, orienting, and moving in response to a chemotactic gradient. Using a retroviral vector, we transduced PLB-985 cells with a GFP-tagged version of a receptor for C5a (hereafter termed the C5aR), a component of complement that is well established as a chemoattractant for neutrophils (Gerard and Gerard, 1991). This approach allows, for the first time, direct observation of a chemoattractant receptor during migration of living neutrophils.

MATERIALS AND METHODS

Materials

[^{125}I]-C5a was from New England Nuclear (Boston, MA). The polyclonal anti-C5aR antibody (Morgan *et al.*, 1993), raised against an amino acid sequence (residues 9–29) near the amino terminus of the human C5aR, was a gift from J.A. Ember and T.E. Hugli (Scripps, San Diego, CA). The Flag-tagged human C5aR cDNA in pCDM8 was a gift from C. Gerard (Harvard Medical School, Boston, MA). CalPhos Maximizer and the GFP fusion vector pEGFP-N3 were from CLONTECH (Palo Alto, CA). 1,1′-Dioctadecyl-3,3,3′,3′-tetramethyllindodicarbocyanine perchlorate (DiD) was from Molecular Probes (Eugene, OR). Texas Red-conjugated goat anti-rabbit IgG was from Jackson Immunoresearch Laboratories (West Grove, PA). Monoclonal GFP antibody was from CLONTECH. Vectashield antifade mounting medium was from Vector Laboratories (Burlingame, CA). Immersion oil (n = 1.518) was from R.P. Cargille Laboratories (Cedar Grove, NJ). Photoetched grid coverslips 1916–92525 were from Bellco Glass (Vineland, NJ). The amphotropic packaging cell line PA317 was from the American Type Culture Collection (Manassas, VA). The myeloid leukemia cell line PLB-985 was a gift from Arie Abo (Onyx Pharmaceuticals, Richmond, CA). The Ψ2 packaging cell line and the pLNCX retroviral vector were gifts from J. Michael Bishop (University of California San Francisco, San Francisco, CA). Polybrene, human recombinant complement C5a, and fMLP were from Sigma Chemical (St. Louis, MO). The carboxy-terminal agonist analogue of C5a, *N*-Met-Phe-Lys-ProdCha-Cha-dArg (ChaCha) (Konteatis *et al.*, 1994) was a gift from Josh Trueheart (Cadus Pharmaceuticals, Tarrytown, NY). G-418 was from Grand Island Biological (Grand Island, NY). All other cell culture reagents were from the Cell Culture Facility (University of San Francisco, San Francisco, CA).

Cell Culture

HEK293 cells and PA317 cells were grown in DMEM supplemented with 10% FBS, 100 U/ml penicillin, and 100 μg/ml streptomycin G. For Ψ2 cells, calf serum was used. PLB-985 cells were grown in RPMI 1640 supplemented with 25 mM HEPES, 10% FBS, 100 U/ml penicillin, 100 μg/ml streptomycin G, 50 μg/ml gentamicin and 2.5

μg/ml fungizone. For differentiation, PLB-985 cells were plated at a density of 0.1×10^6 cells/ml and grown for 4 d until they reached a density of $\sim 1.5 \times 10^6$ cells/ml. Cells (2 ml) were then diluted with 16 ml fresh medium (lacking G-418, gentamicin, and fungizone), and 2 ml of a 13% stock solution of DMSO was added to the cell suspension. Cells were propagated for 6 or 7 d without changing the medium. Under these conditions, cells remained subconfluent, and differentiation was optimal, as determined by superoxide production (Iiri *et al.*, 1995). Conditioned medium was collected from PLB-985 cells plated at a density of 1×10^5 cells/ml and grown for 3 d until they reached a density of $\sim 8 \times 10^5$ cells/ml. Cells were spun down, and the medium was harvested and filtered though a 0.22-μm filter.

C5aR–GFP

To create a C5aR–GFP fusion protein, the whole C5aR cDNA in pCDM8 was amplified by PCR between a T7 primer and a C5aR cDNA carboxy-terminal primer, 5′-CGCGATACCGGTACCCACT-GCCTGGGTCTTCTGGGCCATAGTGTC-3′, designed to remove the stop codon and create a *Kpn*I site (underlined bases) for in-frame ligation with the *Kpn*I site of pEGFP-N3, located at the 5′- end of the GFP DNA. The PCR product was cut with *Hin*dIII/*Kpn*I and subcloned into the pEGFP-N3 fusion vector also cut with *Hin*dIII/*Kpn*I. A *Hin*dIII/*Fse*I fragment of the PCR-generated product was replaced by a *Hin*dIII/*Fse*I fragment from the original C5aR cDNA in pCDM8 to circumvent possible mutations in the receptor sequence introduced by PCR. The final ligated product was sequenced though the remaining region generated by PCR.

Generation of Amphotropic Retroviruses

A retroviral approach was used to create a stable population of PLB-985 cells expressing GFP or C5aR–GFP. The C5aR–GFP and GFP DNAs were subcloned into the pLNCX retroviral vector (Miller and Rosman, 1989) under the control of the cytomegalovirus promoter. The retroviral plasmids were transfected into Ψ2 ecotropic packaging cells by calcium/phosphate precipitation. Transiently produced virus was harvested after 48 h and used to transduce amphotropic PA317 packaging cells. Infections were carried out in 8 μg/ml polybrene for 4 h, infected medium was then diluted 1:1 with fresh PA317 culture medium, and cells were incubated an additional 48 h. Transduced PA317 cells were then selected in 0.5 mg/ml of active G-418. After 8–10 d, stable populations of G-418–resistant PA317 cells were established.

Transduction of PLB-985 Cells

PLB-985 cells were cocultured with retrovirally expressing PA317 cells and 8 μg/ml polybrene for 24 h, removed from the PA317 cell monolayer, and plated for 4 h on a new 100-mm culture dish, to separate the PLB-985 cells, which remain in suspension, from contaminating PA317 cells, which adhere to the dish. Transduced PLB-985 cells were selected by incubating an initial concentration of 1×10^5 cells/ml in conditioned medium containing 1.0 mg/ml G-418. Cell medium was changed every other week until confluency was reached ($\sim 1.5 \times 10^6$ cells/ml). Homogeneous populations of GFP- or GFP–C5aR-positive cells were obtained by fluorescence-activated cell sorting (FACS).

Chemotaxis Assays

HEK293 clones expressing the C5aR and C5aR–GFP were generated as described (Neptune and Bourne, 1997). Chemotaxis assays using these cells were performed in 48-well Boyden chambers as described (Neptune and Bourne, 1997).

Binding Assays

PLB-985 cells (2×10^5 cells) were incubated at 4°C for 5 h with various concentrations of [^{125}I]-C5a (400 Ci/mmol, 0.06–3.6 nM) in 200 μl binding buffer containing HBSS, 25 mM HEPES pH 7.4 and 0.1% (wt/vol) bovine serum albumin. Nonspecific binding was defined as the radioactivity bound in the presence of 100 nM nonradioactive C5a. Incubations were terminated by vacuum filtration though presoaked GF/C glass fiber filters (Whatman, Clifton, NJ), followed by rapid washing with 6 ml of ice-cold binding buffer. To determine binding affinities and capacities (K_d and B_{max}), binding data were subjected to nonlinear regression analysis using Prism software (GraphPad Software, San Diego, CA).

Microscopy

Differentiated PLB-985 cells were washed once with 10 ml RPMI 1640/25 mM HEPES and resuspended at a concentration of 3×10^6 cells/ml in modified HBSS (mHBSS) containing 150 mM NaCl, 4 mM KCl, 1.2 mM $MgCl_2$, 10 mg/ml glucose, and 20 mM HEPES, pH 7.2. Cells (3×10^5 in 100 μl) were plated on the center of a sterile no. 1.5 coverslip rimmed with a square agarose spacer 10 mm in length and 1 mm in height. The coverslip was incubated in a humid chamber at 37°C with 5% CO_2 for 20 min, and nonadherent cells were removed by two washes with mHBSS. Cells were stimulated at room temperature, either uniformly or from a point source of chemoattractant delivered with a micropipette. In the latter case, micropipettes were prepared from a borosilicate capillary with an outer diameter of 1.0 mm and an inner diameter of 0.58 mm using a model P-80/PC Flamming Brown Micropipet Puller (Sutter Instruments, Novato, CA) with step 1: heat = 635; velocity = 20; time = 1; step 2: heat = 605; pull = 160; velocity = 75; time = 25. Under these pulling conditions, the tip of the micropipette is sealed. The micropipette was back-filled with a solution of 10 μM fMLP or 100 μM ChaCha in mHBSS and lowered in focus into the center of the microscope's field of view with a micromanipulator (Narishige USA, Greenvale, NY). The micropipette's tip was broken by touching the side of a broken coverslip. When necessary, air bubbles were pushed out of the micropipette tip by applying a small pressure using a microinjection device. Under these conditions, the broken tip of the micropipette was 0.2 μm or less in diameter and produced more dramatic and more reproducible neutrophil chemotaxis toward the micropipette than did commercially available micropipettes with 0.5-μm tips (Eppendorf Femtotips).

All images were acquired with a scientific-grade cooled charged-coupled device on a multiwavelength wide-field three-dimensional microscopy system (Hiraoka *et al.*, 1991) in which the shutters, filter wheels, focus movement, and data collection were all computer driven. Cells were imaged using a 60 × 1.4 N.A. lens (Olympus, Lake Success, NY) and n = 1.518 immersion oil. Differential interference contrast images were acquired with a Nomarski system optimally aligned for our microscope system. For fluorescence imaging of living cells, the GFP and DiD signals were acquired in the FITC and Texas Red channels, respectively, on single optical sections (0.25 μm) near the bottom of cells. These conditions, at our microscope setting, produce partial confocal images of the samples (Hiraoka *et al.*, 1990). For fluorescence imaging of fixed cells, data stacks of immunofluorescent samples were acquired in the FITC and Texas Red channels by moving the stage in successive 0.25-μm focal planes through the sample. Out-of-focus light was removed with a constrained iterative deconvolution algorithm (Agard *et al.*, 1989).

To quantify the relative distribution of receptors within the plasma membrane, DiD and GFP signals were digitally recorded in their respective channels, and total fluorescence intensity of each was determined in five polygons of fixed area, placed at the front and sides of four separate cells. Fluorescence values were divided by the number of pixels, basal fluorescence (based on fluorescence outside the cell) subtracted, and values for the two probes normalized relative to the maximum fluorescence observed in an individ-

ual cell for GFP or DiD. Then the ratio of fluorescence intensity of GFP to that of DiD was calculated for each polygon. Mean ± SEM of the ratios for the 20 polygons (4 cells, 5 polygons in each) was calculated.

Immunoblotting

Cells (5×10^6) were lysed in 500 μl SDS sample buffer, and cell extracts were resolved on 8% polyacrylamide gel and transferred onto polyvinylidene difluoride membranes. GFP and C5aR–GFP were detected by immunoblotting with a monoclonal GFP antibody.

Immunostaining of Cell-Surface Receptors

Differentiated PLB-985 cells were plated as already described on etched grid coverslips, stimulated with a point source of chemoattractant, and fixed for 20 min by flooding with an excess of 3.7% paraformaldehyde in cytoskeleton buffer containing 10 mM HEPES, pH 7.2, 138 mM KCl, 3 mM $MgCl_2$, 2 mM EGTA, and 0.32 M sucrose. The location of cells responding to the micropipette was then recorded on the grid coverslip, which contains 520 alphanumeric coded squares. Cells were then washed twice in phosphate buffered saline, incubated for 20 min in a blocking solution (blotto) containing 50 mM Tris-HCl, pH 7.5, 1 mM $CaCl_2$, and 3% dry milk, followed by a 45-min incubation with a polyclonal anti-C5aR antibody (5 μg/ml in blotto). This antibody competes against C5a for binding to its receptor but not against carboxy-terminal analogues of C5a (Morgan *et al.*, 1993). After three successive washes in a solution containing 25 mM Tris-HCl, pH 7.4, 140 mM NaCl, 2.5 mM KCl, and 1 mM $CaCl_2$, the cells were incubated with Texas Red-conjugated goat anti-rabbit IgG (1:100 dilution in blotto) for 20 min. They were then washed three times, mounted in Vectashield, and sealed on a slide with clear nail polish.

Plasma Membrane Labeling with DiD

Differentiated PLB-985 cells were washed as already described. DiD (5 mg/ml in ethanol) was added to the cell suspension (in mHBSS) to a final concentration of 3.3 μg/ml. Cells were thoroughly mixed with the dye, and 3×10^5 cells (in 100 μl) were plated on each glass coverslip. After an incubation of 20 min at 37°C, cells were washed twice with mHBSS and kept in the dark at room temperature until analysis. After long incubations, DiD labels intracellular membranes to some degree (including pinocytotic vesicles). However, we quantified DiD:GFP ratios (see above) only for fluorescent signals at the plasma membrane.

RESULTS

Responses of PLB-985 Cells to Chemoattractant

Morphological and behavioral responses of differentiated PLB-985 cells to chemoattractant closely resemble those of blood neutrophils. In the experiment shown in Figure 1, a micropipette filled with 10 μM fMLP is positioned in front of three polarized cells. Within 30 sec, cell *a* shows intense ruffling at its leading edge (Figure 1A, arrows; a video of the experiment described in this figure is available on the internet version of this paper, at http://www.molbiolcell.org). In response to successive movements of the pipette (Figure 1, B–F), cell *a* extends new pseudopodia (arrowheads), reorients, and crawls toward the pipette. Repositioning the micropipette near cells *b* and *c* (Figure 1, G and H) causes these cells to respond and extend pseudopodia toward the micropipette, while cell *a* continues to follow. Upon removal of the chemoattractant source (Figure 1I), the three cells retract their pseudopodia but keep their polarized morphology.

After differentiation, 50–75% of the PLB-985 cells are unpolarized in the absence of chemoattractant (Figure 1J) but polarize rapidly in response to a pipette containing chemoattractant (Figure 1, K and L). Some cells in the differentiated population, unlike neutrophils, retract their uropods ineffectively, resulting in the formation of long membrane extensions at their back (Figure 1, cell *a*, panels C–D). In addition, some cells (our unpublished data) show no morphological response to uniform or pipette-delivered chemoattractant; we suspect that such cells are not fully differentiated.

Expression of recombinant genes in PLB-985 cells does not affect the response to a chemotactic gradient (Figure 2; a video of the experiment described in this figure is available on the internet version of this paper, at http://www.molbiolcell.org). Using a retroviral vector, DNA-encoding GFP was transferred into undifferentiated PLB-985 cells. A population of transduced cells, selected for resistance to G-418 (see MATERIALS AND METHODS), was further selected (by FACS) for expression of GFP. GFP expression in this population is robust but varies significantly from cell to cell (compare cells *b*, *d*, and *e*, Figure 2A). In the experiment depicted in Figure 2, five GFP-expressing cells (previously induced to differentiate by exposure to DMSO; see MATERIALS AND METHODS) rapidly extend pseudopodia toward the micropipette delivering fMLP (Figure 2B, arrowheads) and crawl toward it until they meet in the center of the field (Figure 2, C–F).

A Functioning C5aR–GFP Chimera Is Expressed at the Cell Surface

To observe the subcellular distribution of a chemoattractant receptor in living cells, we attached GFP to the carboxy terminus of the human C5aR. Figure 3 shows that the C5aR–GFP chimera can mediate chemotaxis in HEK293 cells and is targeted to the plasma membrane of PLB-985 cells. Because the C5aR is normally present in neutrophils (Gerard and Gerard, 1991), we chose to test the ability of the chimera to mediate chemotaxis in stably transfected HEK293 cells; the C5aR–GFP and the wild-type C5aR mediate chemotaxis over the same range of C5a concentrations (Figure 3, A and B). The C5aR–GFP also supports chemotaxis in stably transfected avian DT-40 pre-B cells (our unpublished data). In PLB-985 cells, immunoblots with anti-GFP antibody show a major 70-kDa band, the size expected for the C5aR–GFP chimera (Figure 3B, lanes 2 and 3). Anti-GFP antibody does not reveal smaller proteins corresponding to the size of free GFP (27 kDa) (Figure 3B).

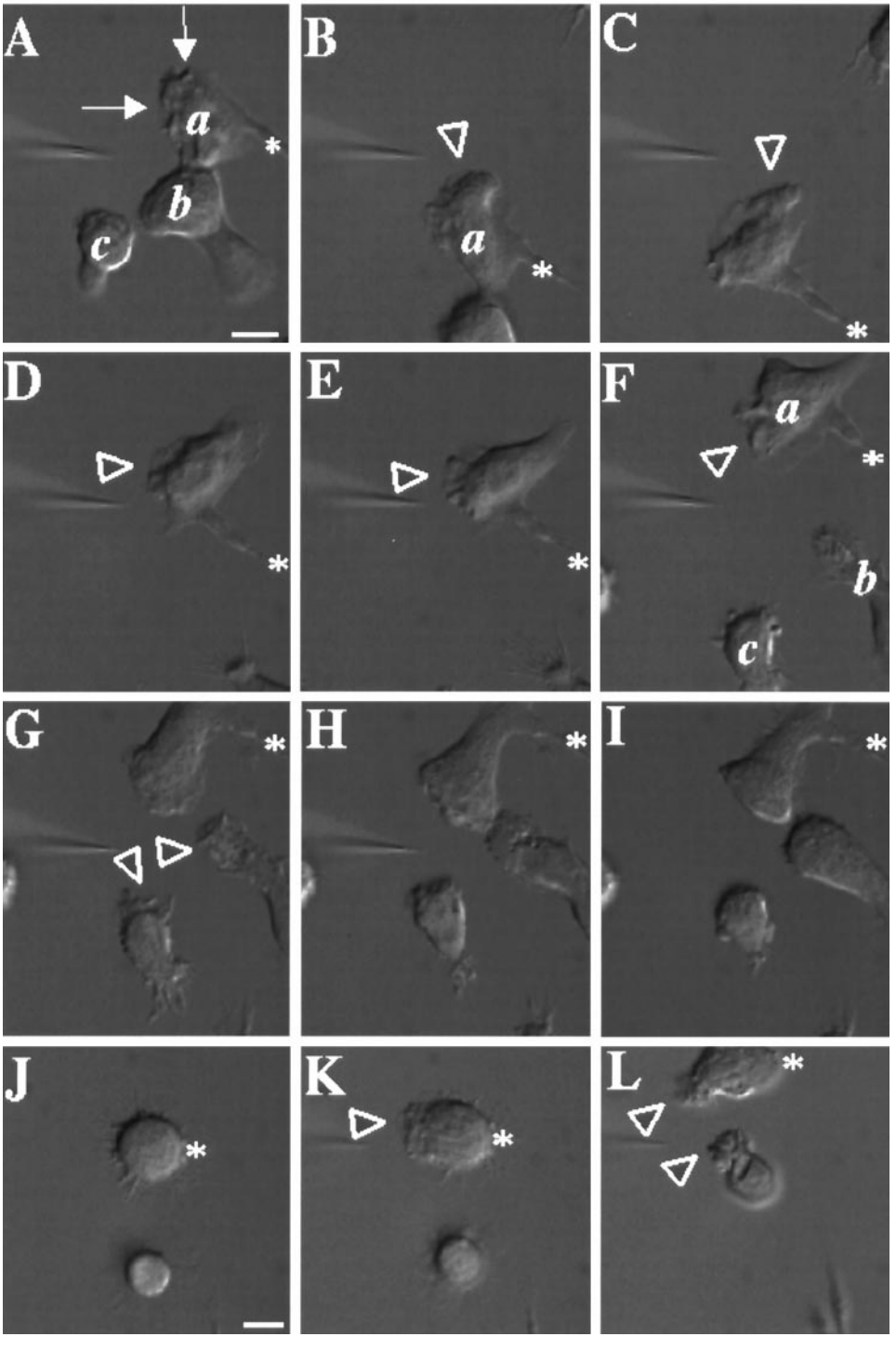

Figure 1. Responses of differentiated PLB-985 cells to a point source of chemoattractant. PLB-985 cells were differentiated by treatment with 1.3% DMSO for 7 d and plated on glass coverslips. Cells were then stimulated with fMLP (10 μM) delivered from a micropipette, and images were recorded every 5 s as described in MATERIALS AND METHODS. Panels A–I show morphological responses after (A) 30, (B) 90, (C) 150, (D) 210, (E) 240, (F) 270, (G) 300, and (H) 360 s of micropipette stimulation; panel I shows the same cells 90 s after removal of the micropipette. Panels J–L show responses of nonpolarized cells after (K) 30 and (L) 140 s exposure to fMLP in the micropipette. Arrows point to chemoattractant-stimulated membrane ruffles. Arrowheads point to newly formed or reorienting pseudopodia. Asterisks indicate stable points of reference in panels A–I and J–L, respectively, to allow the reader to appreciate movement of the micropipette. This session is representative of three similar observations. Bar, 10 μm. A video of the experiment described in this figure is available on the internet version of this paper, at http://www.molbiolcell.org.

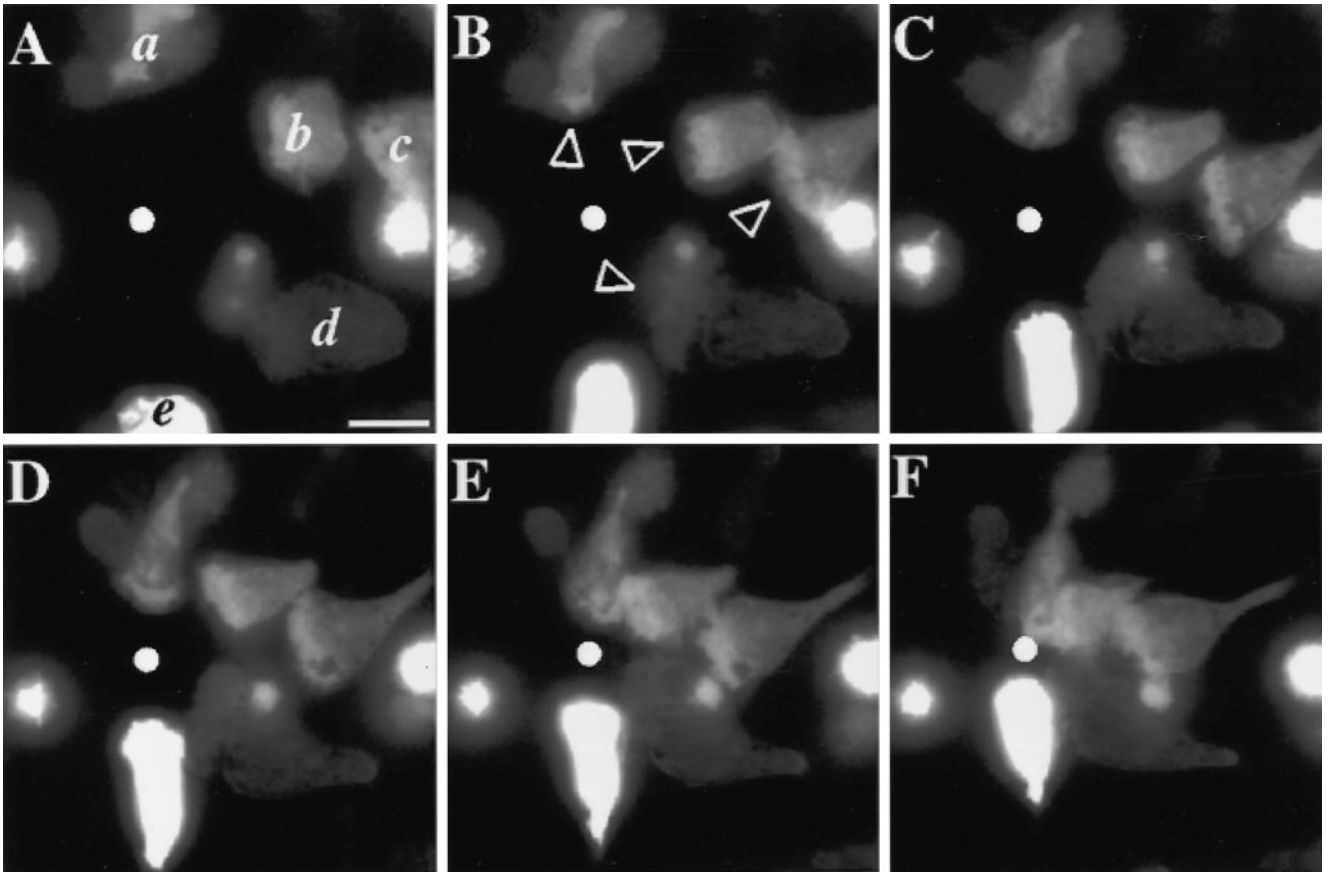

Figure 2. Chemotactic behavior of PLB-985 cells stably expressing GFP introduced by a retroviral vector. Cells were infected, selected in G-418, and sorted by FACS for GFP fluorescence, as described in MATERIALS AND METHODS. GFP-expressing cells were differentiated in 1.3% DMSO for 7 d and plated on glass coverslips. Cells were then stimulated with fMLP (10 μM) delivered from a micropipette (white dot), and images were recorded every 5 s, under pseudoconfocal conditions, as described in MATERIALS AND METHODS. Panels A–F show responses after (A) 0, (B) 60, (C) 120, (D) 180, (E) 240, and (F) 300 s. Arrowheads point to pseudopodia advancing in response to the agonist. This session is representative of two similar observations. Bar, 10 μm. A video of the experiment described in this figure is available on the internet version of this paper, at http://www.molbiolcell.org.

The C5aR–GFP chimera is expressed on the plasma membrane of PLB-985 cells. Using a retroviral vector, the gene encoding C5aR–GFP was transferred into nondifferentiated PLB-985 cells. Transduced cells were then selected and GFP-positive cells sorted by FACS (see MATERIALS AND METHODS). As expected for a membrane-bound protein, the C5aR–GFP fluorescent signal in differentiated cells is enriched at the cell periphery (Figure 4, A and A′). Saturation-binding experiments performed with [^{125}I]-C5a reveal that expression of the C5aR–GFP chimera increased maximal binding of C5a at the cell surface by ~60%, relative to cells expressing the endogenous C5aR (Figure 3C): K_d and B_{max} values (mean ± SD of 3 determinations) were 0.51 ± 0.06 nM and 63,900 ± 7500 sites/cell for C5aR-GFP–expressing cells, and 0.57 ± 0.23 nM and 40,900 ± 6100 sites/cell for cells expressing GFP alone (not fused to the C5aR). Both B_{max} values are within the range previously reported for the C5aR of neutrophils (Huey and Hugli, 1985; Drapeau *et al.*, 1993). Fluorescence intensities of individual cells, however, vary by as much as 10-fold, as determined by FACScan analysis (our unpublished data). Thus the number of C5aR–GFP molecules in the PLB-985 cells we examined ranges from ~8000 to ~80,000 per cell. Nonetheless, the cell-surface location of the C5aR–GFP protein on moving PLB-985 cells does not depend on the level of its expression (see Figure 5, compare cells *a* and *d*).

Distribution of the C5aR-GFP in PLB-985 Cells

Exposure of PLB-985 cells to a uniform concentration of C5a causes agonist-induced internalization of a portion of some C5aR-GFP molecules, but the distribution of receptors at the cell surface remains uniform even when the cells polarize in response to the chemoattractant. In the experiment summarized in Figure 4,

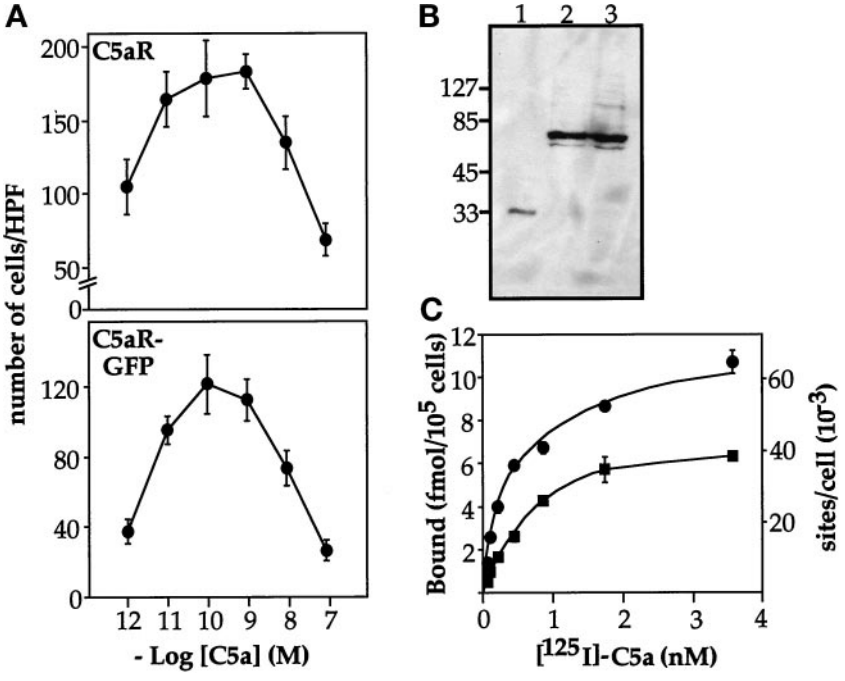

Figure 3. Characterization of the C5aR-GFP chimera. (A) C5aR–GFP can mediate chemotaxis. HEK293 cells stably expressing either the C5aR or the C5aR–GFP fusion protein were subjected to a migration assay in a 48-well Boyden chamber, as described previously (Neptune and Bourne, 1997). At the end of the assay, cells adhering to the lower side of the porous filter were fixed, stained, and counted using a microscope. Results are expressed as the number of cells counted in a high-power field (HPF) (200×) and correspond to the mean ± SD of four determinations. Similar results were obtained in four other experiments. Absolute numbers of migrated cells in the experiment shown do not reflect different abilities of the two cell types to migrate toward C5a; instead, the absolute numbers reflect the numbers of each cell type used in each well (22,500 and 37,500 cells expressing the C5aR–GFP or the C5aR, respectively). (B) Integrity of the C5aR–GFP fusion protein in differentiated PLB-985 cells. PLB-985 cells were transduced with a retrovirus carrying C5aR–GFP as described in MATERIALS AND METHODS. Transduced cells were selected and GFP-positive cells were sorted by FACS. Cell extracts were prepared from 5×10^6 differentiated cells as described in MATERIALS AND METHODS, resolved on 8% polyacrylamide, and transferred onto a polyvinylidene difluoride membrane. GFP and the C5aR–GFP were then revealed with a monoclonal GFP antibody. Lane 1, extract from 10^5 GFP-expressing cells; lanes 2 and 3, extracts from two different aliquots, each representing 3×10^5 C5aR-GFP–expressing cells. (C) Binding of [^{125}I]-C5a to PLB-985 cells. Differentiated GFP-expressing cells (squares) and C5aR-GFP–expressing cells (circles) were incubated at 4°C for 5 h with the indicated concentrations of [^{125}I]-C5a (0.06–3.6 nM). Nonspecific binding was evaluated in the presence of 100 nM nonradioactive C5a. Incubations were terminated by rapid filtration though GF/C filters. In the experiment shown, nonlinear regression analysis of the binding data yielded B_{max} values of 68,400 sites/cell and 47,600 sites/cell for C5aR–GFP and GFP-expressing PLB-985 cells, respectively. Similar results were obtained in two additional experiments.

receptor distribution in five cells is recorded in living cells under pseudoconfocal conditions (Hiraoka *et al.*, 1990) (a video of the experiment described in this figure is available on the internet version of this paper, at http://www.molbiolcell.org). Within 56 s of C5a treatment, clusters of C5aR–GFP begin to form at the plasma membrane (Figure 4, C and C′, arrows). Later time points (Figure 4, D and E) reveal considerable internalization of C5aR–GFP, in addition to a dramatic change in cell morphology. Cells increase in size, owing to agonist-induced spreading and increased adhesion on the glass coverslip (Figure 4, D and E). After exposure to C5a for 3 min, four of the five cells clearly exhibit front-tail polarity, and internalized receptors are concentrated in their uropods (Figure 4, F and F′, arrowheads). C5aR–GFP remaining at the cell surface, however, remains uniformly distributed through the plasma membrane, qualitatively (Figure 4, F and F′) and as indicated by a scan of fluorescence intensity (Figure 4G).

Expression of the C5aR–GFP does not impair the ability of PLB-985 cells to respond to chemoattractant (Figure 5; a video of the experiment described in this figure is available on the internet version of this paper, at http://www.molbiolcell.org). In this experiment, visualized under pseudoconfocal conditions, cells orient and move toward a point source of a C5aR agonist, ChaCha (Konteatis *et al.*, 1994), delivered by micropipette. Their behavior mimics in detail that described for neutrophils under similar circumstances (Zigmond, 1974; Gerisch and Keller, 1981). The micropipette is first positioned in the middle of a field containing five cells (Figure 5A). Within 44–110 s, all cells in the field show clear responses to the ChaCha gradient (Figure 5, B and C). Cell *a*, which was already polarized toward the center of the cell cluster before stimulation (Figure 5A), now exhibits extensive ruffling at its front; cells *c* and *d* are clearly polarized and also exhibit ruffling at their fronts (Figure 5B, arrowheads). The back of cell *b*, characterized by its retraction fibers (Figure 5A, filled arrowhead), transforms into a new leading edge that moves toward the micropipette, while cell *e* turns its front toward the micropipette (Figure 5B). At later time points, all cells in the field converge and crawl toward the micropipette (Figure 5, D–F); additional cells, not in the field at the beginning of the experiment, also make their way up the ChaCha gradient (Figure 5D).

Figure 5 also shows that C5aR–GFP fluorescence remains uniformly distributed on the surface of cells

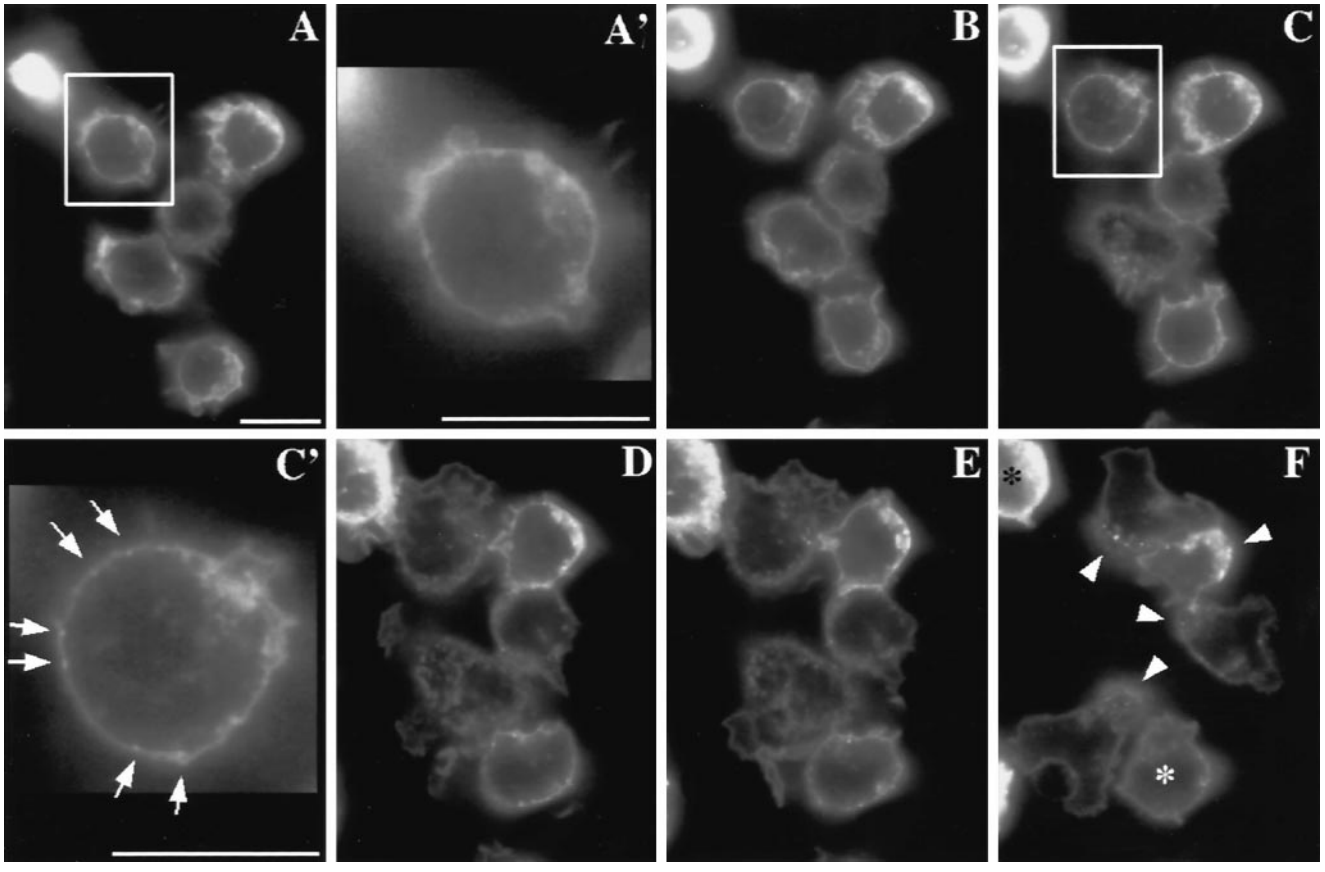

Figure 4. C5aR–GFP dynamics after stimulation of PLB-985 cells with a uniform concentration of C5a. C5aR-GFP–expressing PLB-985 cells were differentiated with 1.3% DMSO, plated on glass coverslips, and exposed to a uniform concentration (20 nM) of C5a in mHBSS; images were recorded every 2 s, under pseudoconfocal conditions, as described in MATERIALS AND METHODS. Responses are shown after (A) 0, (B) 28, (C) 56, (D) 140, (E) 168, and (F) 308 s. Panels A′ and C′ show magnifications of the cells indicated in panels A and C, respectively. Panel F′ shows a magnification of panel F. Panel G shows a fluorescence intensity scan analysis of the cell in the lower left corner in panels F and F′. Arrows point to agonist-stimulated receptor patches. Arrowheads (in F and F′) point to internalized receptors located in the uropod of polarized cells. The asterisks in panel F indicate cells that spread but did not clearly develop a polarized morphology after stimulation. This session is representative of three similar observations. Bar, 10 μm. A video of the experiment described in this figure is available on the internet version of this paper, at http://www.molbiolcell.org.

orienting and moving toward the ChaCha-containing micropipette, just as in the case of cells exposed to a uniform concentration of chemoattractant (see Figure 4). The agonist delivered by micropipette also induces accumulation of internalized C5aR–GFP in the uropods of polarized cells (Figure 5F, red arrowheads) within a time scale similar to that seen in uniformly stimulated cells (Figure 4). Nonetheless, most cells show no relative increase of fluorescence intensity anywhere on the cell surface, not even at the leading edge. Trailing portions of certain cells show an apparent decrease in fluorescent signal (Figure 5, C and E, arrows), but focusing up and down showed that this appearance reflects a difference in cell shape at the trailing edge, where the cell flattens and terminates in retraction fibers (see Figure 1A, cells *a* and *b*). Consequently, focusing on the front and midregion of cells causes a loss of fluorescence intensity at the back.

C5aR–GFP Fluorescence Is Proportional to Membrane Surface

By itself, the C5aR–GFP fluorescent signal may not reflect with precision the density of receptor molecules per unit area of plasma membrane. For example, we sometimes observed an apparent enrichment of C5aR–GFP fluorescence at the anterior poles of moving cells (see Figure 5C, cells *b* and *c*), and therefore asked whether this resulted from an increased density of receptors or from an increased amount of plasma membrane, which might be folded more extensively at a cell's leading edge. The experiments shown in Figures 6 and 7 indicate that the latter explanation is correct.

In the three cells shown in Figure 6, each stimulated by a point source of ChaCha, plasma membranes are labeled with a membrane probe, DiD. C5aR-GFP and DiD signals are alternatively recorded, in the FITC and

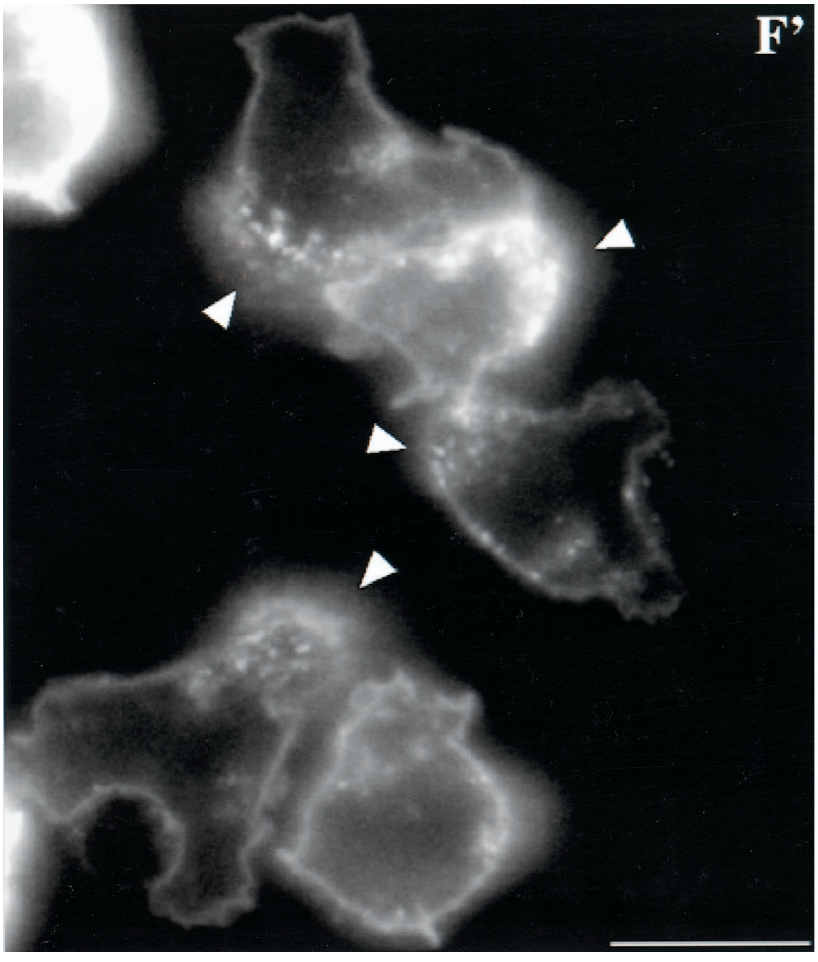

Figure 4 (cont).

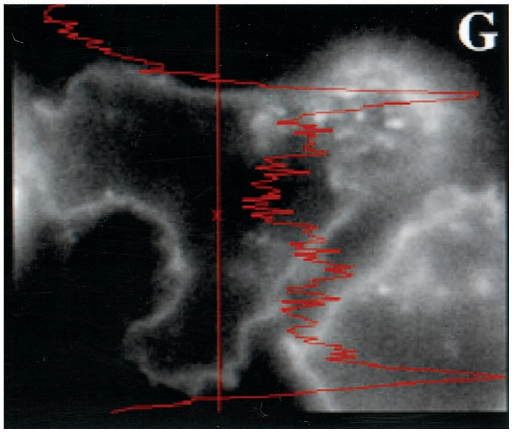

Texas Red channels, respectively. The cells in panels A and C crawl toward the micropipette (shown by the white dot) while the cell in panel B polarizes toward it. At this magnification it is possible to appreciate the complexity of the fluorescent signal at the leading edge (Figure 6, arrows), which reflects ruffles or folds of the plasma membrane caused by dramatic reorganization of the actin cytoskeleton beneath it (Weiner, Servant, Sedat, and Bourne, manuscript in preparation). Under these conditions, the cell in panel A and (to a lesser extent) cells in panels B and C exhibit greater C5aR–GFP fluorescence at their anterior poles where the membrane folds are more complex. DiD fluorescence is also higher at the anterior poles of the cells; indeed, distributions of the C5aR–GFP and DiD signals are superimposable. We infer that the apparent increases in C5aR–GFP concentration reflect increases in relative abundance of plasma membranes, rather than preferential accumulation of receptors, at the leading edge. Quantification of the GFP and DiD signals in 20 patches of membrane (see MATERIALS AND METHODS) revealed a ratio of fluorescence intensities for the two probes (GFP:DiD) of 1.08 $\pm$ 0.05 (mean $\pm$ SEM of 20 determinations performed in 4 separate cells migrating toward chemoattractant). This ratio does not differ significantly from 1.0; we cannot, however, rule out a very small change ($<$ 8%) in receptor distribution.

To test this inference more stringently, we examined C5aR–GFP and DiD distribution in a different way (Figure 7). In this experiment, the C5aR–GFP and DiD signals are acquired on a fixed cell in successive 0.25-μm focal planes through the sample, and out-of-focus light is removed with a constrained iterative deconvolution algorithm (Agard *et al.*, 1989). Maximum intensity projections of all the three-dimensional data stacks from a polarized cell clearly show membrane enrichment and concomitant enrichment of receptor density at the leading edge (Figure 7A, arrow). Figure 7B shows a single focal plane of the cell in panel A. Once again, the leading edge shows parallel enrichment of DiD and C5aR–GFP fluorescence in a pattern that suggests the existence of complex folds even within a thin section. Together these results indicate that asymmetric distribution of plasma membrane folds can alter the apparent distribution of a mem-

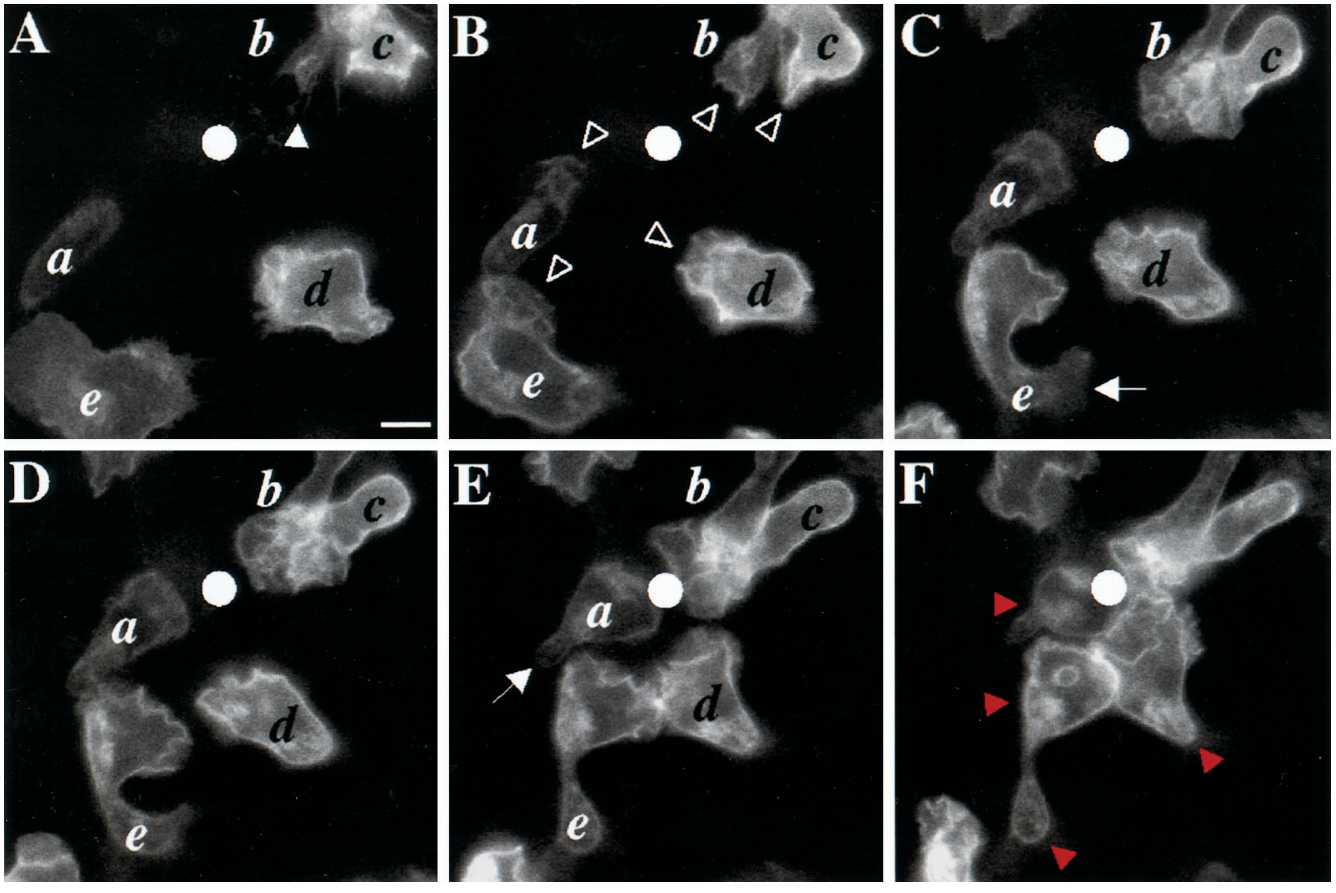

Figure 5. C5aR-GFP dynamics after stimulation of PLB-985 cells with a point source of ChaCha delivered from a micropipette. C5aR-GFP-expressing cells were differentiated with 1.3% DMSO and plated on glass coverslips. Cells were then stimulated with ChaCha (100 μM) delivered from a micropipette, and images were recorded every 2 s, under pseudoconfocal conditions, as described in MATERIALS AND METHODS. Responses are shown after (A) 0, (B) 44, (C) 110, (D) 154, (E) 176, and (F) 220 s of micropipette stimulation (white dot). The closed arrowhead in panel A points to the retraction fibers of cell *b*. Open arrowheads (panel B) point to ruffles at the leading edges of locomoting cells. Arrows in panels C and E point at the back of polarized cells. Red arrowheads (panel F) point to internalized C5aR–GFP. This session is representative of three similar observations. Bar, 10 μm. A video of the experiment described in this figure is available on the internet version of this paper, at http://www.molbiolcell.org.

brane protein detected by fluorescence microscopy, which has been extensively utilized to localize chemoattractant receptors on leukocytes (Schmitt and Bultmann, 1990; McKay *et al.*, 1991; Nieto *et al.*, 1997). The results also point to a potential limitation of confocal microscopy: apparent enrichment of a protein may reflect tight folds of the plasma membrane, rather than changes in concentration of the protein per square micron of membrane.

Receptors Accessible to the Ligand Are Also Uniformly Distributed

The experiment shown in Figure 8 rules out an alternative mechanism that neutrophils might use to amplify a chemotactic gradient. In this hypothetical mechanism, intensity of the extracellular signal is increased at the front because receptors at the back of the cell are sequestered in a compartment not accessible to ligand, but located just under the plasma membrane; if so, C5aR–GFP would appear uniformly distributed, even though a larger fraction of the receptors at the front of the cell would be able to detect the chemoattractant. To test the hypothesis, C5aR-GFP–expressing cells are stimulated with a point source of ChaCha and fixed, and receptors are assessed both by the C5aR-GFP fluorescent signal and with an antibody raised against a peptide corresponding to the extracellular amino terminus of the C5aR (Morgan *et al.*, 1993). Because this antibody does not compete against C5a analogues for binding to the C5aR (Morgan *et al.*, 1993), it is possible to localize cell surface receptors after stimulation with ChaCha. Figure 8 shows a C5aR-GFP–expressing cell fixed while crawling toward ChaCha, delivered by a micropipette (the arrow-

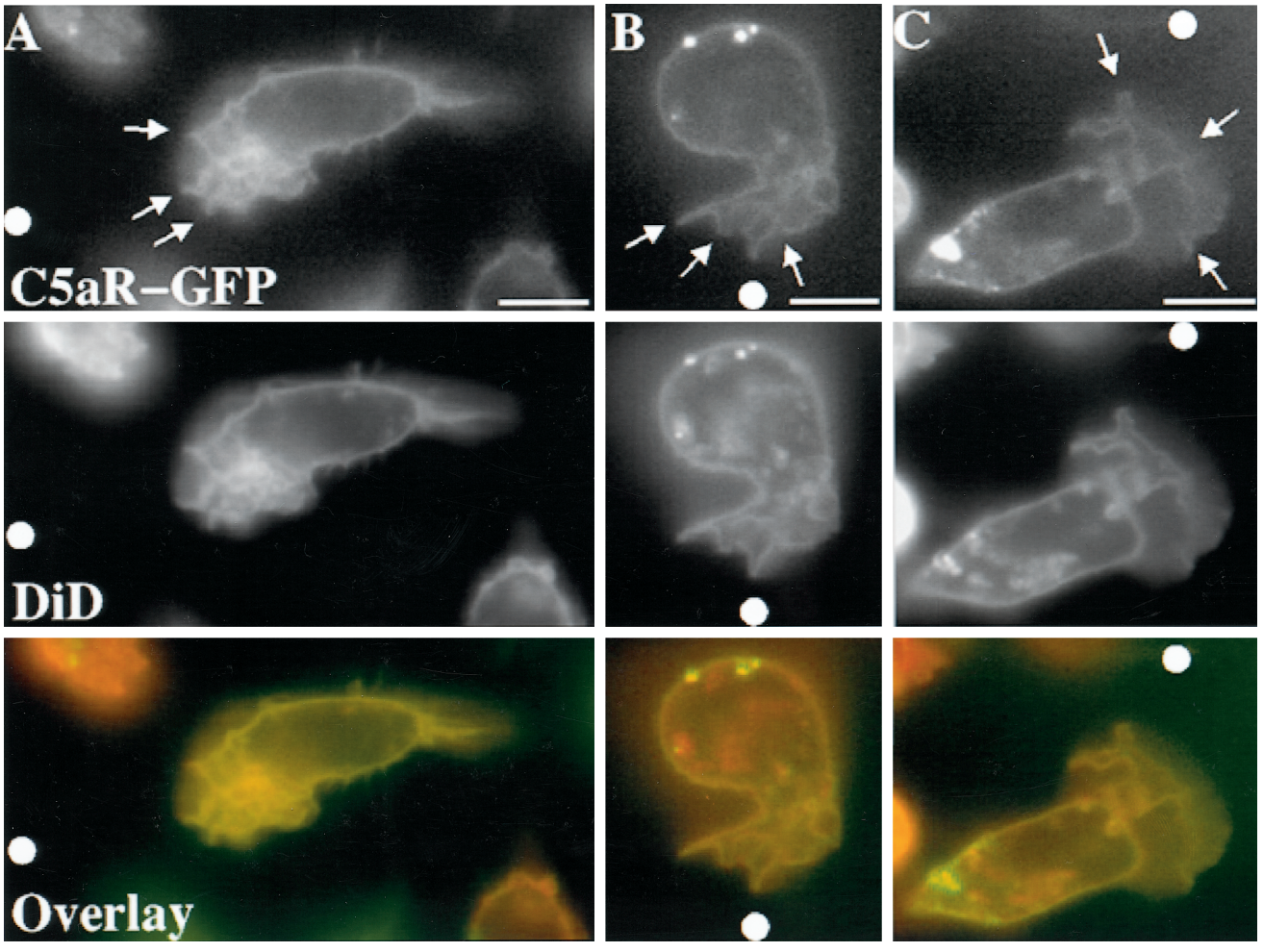

Figure 6. Localization of C5aR–GFP relative to the plasma membrane of moving PLB-985 cells. C5aR-GFP–expressing cells were differentiated with DMSO 1.3%, labeled with DiD, and plated on glass coverslips. Cells were then stimulated with ChaCha (100 μM) delivered from a micropipette. Under pseudoconfocal conditions, the GFP and DiD signals were alternatively recorded in the FITC and Texas Red channels, respectively, as described in MATERIALS AND METHODS. Single cells, from three different experiments, are shown crawling toward the source of ChaCha (white dot). Arrows point to the ruffling fronts of the cells. Bar, 10 μm.

head indicates the direction of migration). Neither the fluorescence specific for the anti-C5aR antibody nor that emitted by C5aR–GFP is enriched at the surface of the cell's leading edge, compared with the back. The C5aR–GFP and the antibody signals overlap, with the exception of the intracellular pool of internalized C5aR–GFP (overlay, arrows).

DISCUSSION

Many investigators have sought to identify and dissect the working parts of the sophisticated guiding system that neutrophils use to find bacteria at sites of infection (Devreotes and Zigmond, 1988; Downey, 1994; Perez, 1994; Bokoch, 1995; Prossnitz and Ye, 1997). Two kinds of observations suggest that this system depends, in part, upon relatively enhanced sensitivity to chemoattractant of the crawling neutrophil's leading edge. First, such cells tend to preserve the same leading edge, often preferring—like cell *e* in Figure 5, above—to turn toward an incoming new chemotactic gradient rather than to form a new front (Zigmond, 1977; Zigmond *et al.*, 1981). Second, neutrophils crawl up a very shallow gradient with little apparent deviation from a straight course, even when the concentration of chemoattractant at the leading edge is only 1% greater than that at the cell's trailing edge. Together, these findings indicate that asymmetric sensitivity of the guidance system itself accompanies the polarized morphology of a neutrophil. An attractive explanation (Zigmond, *et al.*,

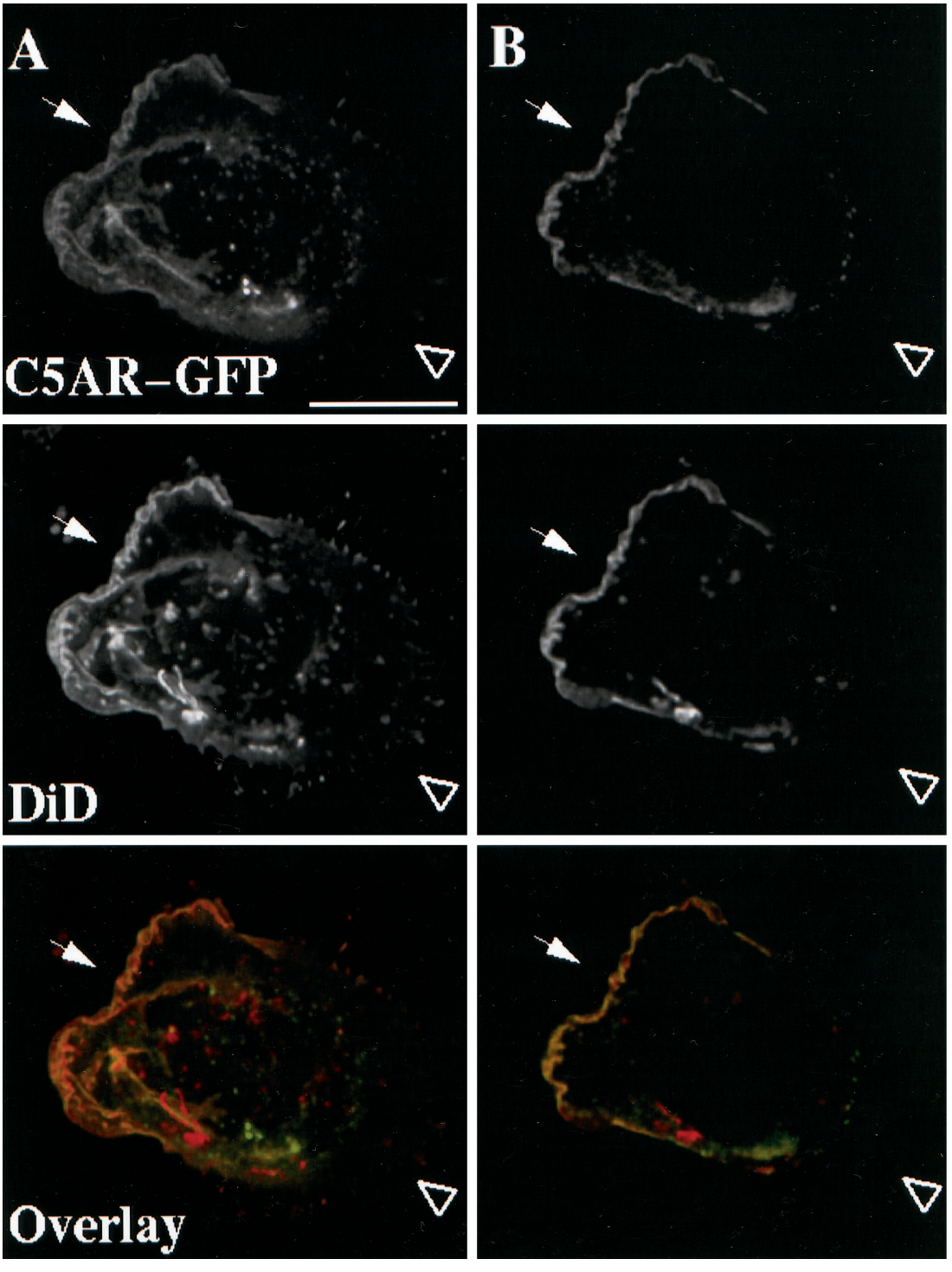

Figure 7. Localization of C5aR–GFP relative to the plasma membrane of fixed PLB-985 cells. C5aR-GFP–expressing cells were differentiated with 1.3% DMSO, labeled with DiD, and plated on glass coverslips. Cells were then stimulated with a uniform concentration (20 nM) of C5a for 3 min at room temperature and fixed. The GFP and DiD signals were acquired alternatively in the FITC and Texas Red channels, respectively, as described in MATERIALS AND METHODS in successive 0.25-μm focal planes through the sample; out-of-focus light was removed with a constrained iterative deconvolution algorithm (Agard *et al.*, 1989). (A) Maximum intensity projections of three-dimensional data stacks from a polarized DiD-stained, C5aR-GFP–expressing-cell. (B) A single focal plane of the cell in panel A. The arrow and arrowhead point to the front and the back of the cell, respectively. Bar, 10 μm.

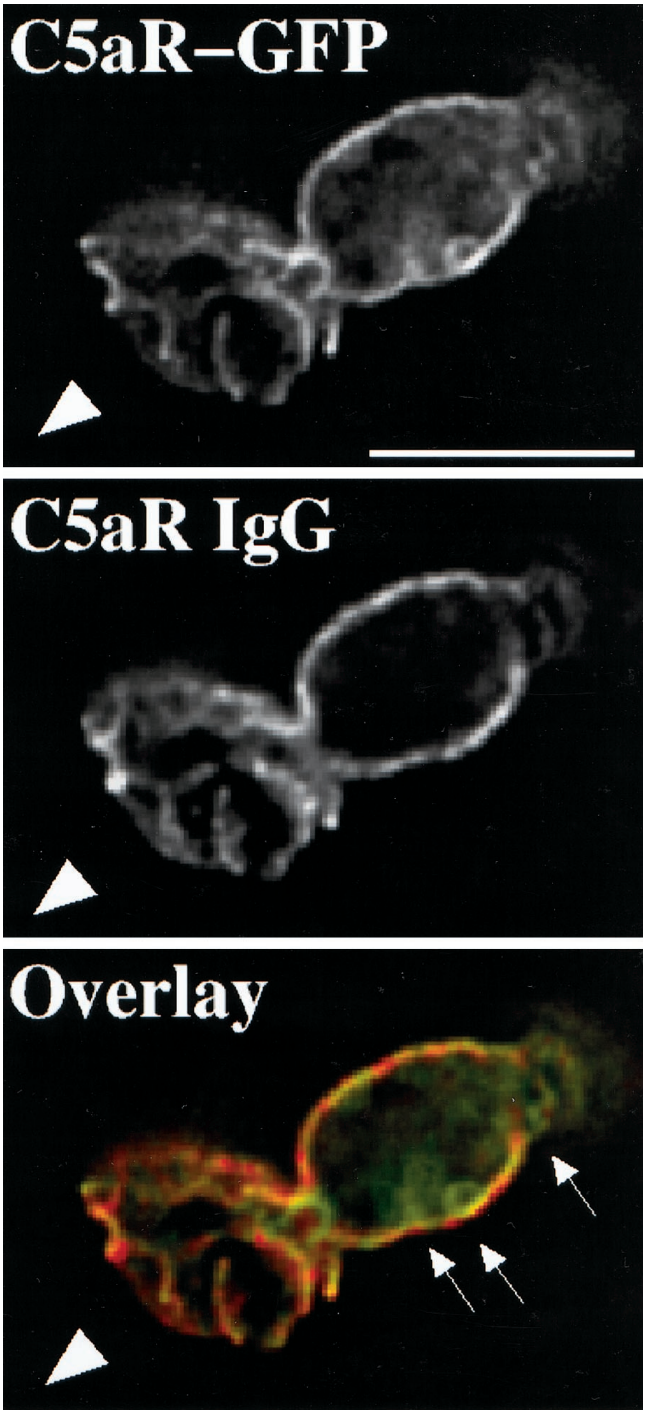

Figure 8. Immunostaining of cell-surface C5aRs. C5aR-GFP–expressing cells were differentiated with 1.3% DMSO and plated on glass-etched grid coverslips. Cells were stimulated with a point source of ChaCha (100 μM) delivered by a micropipette and fixed. Locations of cells responding to the micropipette were recorded, and immunofluorescence of surface C5aR was assessed as described in MATERIALS AND METHODS. The GFP and IgG signals were acquired alternatively in the FITC and Texas Red channels, respectively, as described in MATERIALS AND METHODS, in successive 0.25-μm focal planes through the sample; out-of-focus light was removed with a constrained iterative deconvolution algorithm (Agard *et al.*, 1989). Images represent a single 0.25-μm focal plane near the bottom of the cell. The arrowhead indicates the direction of migration. Arrows point to internalized clusters of C5aR–GFP. These results were reproduced in one additional independent experiment. Bar, 10 μm.

1981; Cassimeris and Zigmond, 1990) for increased sensitivity and persistence of the neutrophil's leading edge is that the chemoattractant receptors themselves accumulate at a higher concentration at the front of the cell. To our knowledge, the present study is the first to test this hypothesis in living neutrophils engaged in chemotaxis. Our results, with differentiated PLB-985 cells expressing a GFP-tagged C5aR, indicate that this hypothesis is not correct. Instead, our results agree with observations in cells of a unicellular organism, *Dictyostelium discoideum*: receptors for cAMP, a chemoattractant for this organism, maintain an even distribution throughout the cell surface during chemotaxis toward a pipette containing cAMP (Xiao *et al.*, 1997).

Here we discuss the relevance of PLB-985 cells for understanding neutrophil chemotaxis, discrepancies between our findings and previous reports, and potential mechanisms that could explain increased sensitivity of the leading edge to chemoattractant, without invoking differential distribution of receptors.

PLB-985 Cells as a Model for Neutrophil Behavior

The PLB-985 cell line was established from cells in the peripheral blood of a patient with acute nonlymphocytic leukemia (Tucker *et al.*, 1987). Growth of these cells in the presence of DMSO induces granulocytic maturation, indicated by morphology, histochemical staining, production of superoxide anions, and increased synthesis of the primary granule proteinases, elastase and cathepsin G (Dana *et al.*, 1998). PLB-985 cells differentiated in the presence of DMSO provide an accurate model for studying neutrophil chemotaxis, as indicated by the following evidence: first, such cells behave like neutrophils when challenged with either a uniform concentration or a gradient of chemoattractant (Figures 1, 2, 4, and 5). Exposed to a uniform concentration of chemoattractant, PLB-985 cells adhere and spread on glass coverslips; some cells then polarize in random directions, much like neutrophils (Davis, *et al.*, 1982; Sullivan, *et al.*, 1984; Walter and Marasco, 1984; Cassimeris and Zigmond, 1990; McKay *et al.*, 1991; Gray *et al.*, 1997). In contrast—again like neutrophils—differentiated PLB-985 cells orient themselves toward and then crawl up the gradient of chemoattractant delivered by micropipette, and retract their pseudopodia when the source is removed.

Several observations indicate that our fluorescent receptor probe, the C5aR–GFP protein, accurately re-

flects behavior of endogenous receptors for C5a and other chemoattractants on the neutrophil surface. The fluorescent protein, GFP, has been fused to many proteins, including G protein-coupled receptors, as a tool for assessing their localization and fate in living cells (Sengupta, *et al.*, 1996; Barak *et al.*, 1997a,b; Tarasova, *et al.*, 1997; Xiao *et al.*, 1997). C5aR–GFP functions indistinguishably from the wild-type C5aR in stably transfected HEK293 cells, where it mediates chemotaxis over the same range of C5a concentrations (Figure 3). C5aR–GFP functions normally in PLB-985 cells also, at least with respect to its ability to undergo rapid agonist-induced internalization (Figures 4, 5, 7, and 8), as is the case in other cells for a number of G protein-coupled receptors fused to GFP (Barak *et al.*, 1997b; Tarasova, *et al.*, 1997). Moreover, C5aR-GFP is targeted to its appropriate location at the plasma membrane of PLB-985 cells, producing a peripheral fluorescent signal that coincides perfectly with that of the fluorescent signal of a plasma membrane probe, DiD (Figures 6 and 7). Finally, it is unlikely that expression of the recombinant C5aR substantially alters sensitivity of PLB-985 cells to C5a ligands, because cell surfaces of these cells display only 60% more C5a-binding sites than do those of control cells expressing GFP alone (Figure 3).

Behavior of C5aR–GFP Compared with Other Chemoattractant Receptors

Before discussing differences between our findings and those of others, we should first note that in several respects the C5aR–GFP fusion protein precisely mimics behavior reported for several other chemoattractant receptors. To infer behavior of chemoattractant receptors in living neutrophils, previous investigations used fluorescently modified ligands, including *N*-formyl peptides and C5a (Janeczek *et al.*, 1989; Schmitt and Bultmann, 1990; Van Epps, *et al.*, 1990; Johansson *et al.*, 1993). Before receptors are internalized, these fluorescent ligands aggregate into patches on the neutrophil membrane (Janeczek, *et al.*, 1989; Van Epps, *et al.*, 1990; Johansson, *et al.*, 1993); similarly, C5aR–GFP forms clusters at the plasma membrane shortly after stimulation with C5a (Figure 4C′). After clustering at the plasma membrane, fluorescent *N*-formyl peptides are internalized and accumulate in the uropods of polarized neutrophils (Schmitt and Bultmann, 1990); similarly, after plasma membrane clusters are observed, C5aR–GFP internalizes and accumulates in uropods (Figure 4, F and F′). Finally, fluorescent fMLP ligands accumulated in the uropods of polarized cells translocate from the uropods to the perinuclear region of neutrophils (Schmitt and Bultmann, 1990); similarly, some internalized C5aR-GFP eventually moves to the perinuclear region of PLB-985 cells (Figure 5F, cell E, red arrowheads and our unpublished data). Thus behavior of the C5aR–GFP molecule closely resembles receptor behavior inferred from studies with fluorescent ligands.

Our observation that the C5aR remains uniformly distributed on the surface of neutrophils during chemotaxis is not in accord with several previous reports that chemoattractant receptors cluster at the leading edge of neutrophils (Walter and Marasco, 1984; Schmitt and Bultmann, 1990; McKay *et al.*, 1991) or T lymphocytes (Nieto *et al.*, 1997). Unlike our experiments, these investigations either tracked fluorescently tagged ligand (rather than the receptors themselves) in real time or used antibodies or radiolabeled ligands to detect receptors in fixed cells. Moreover, none of these studies asked whether the increased fluorescent or radioactive signal at the anterior pole of a polarized cell represents an increased number of receptor molecules per unit area of membrane or simply reflects complex membrane folding at the front. An increased "concentration" of plasma membrane at the leading edge, probably produced by complex membrane folds, could produce the illusion of a higher concentration of membrane receptors, even in confocal microscopy, as suggested by comparing the C5aR-GFP and DiD patterns of Figures 6 and 7. Instead, our observations suggest that during chemotaxis C5aR–GFP behaves very like an inert probe of membrane concentration, and is not concentrated, per unit of cell surface, at the leading edge or anywhere else. In keeping with this inference, two studies (McKay *et al.*, 1991; Nieto *et al.*, 1997) showed that the apparent redistribution of chemoattractant receptors to the leading edge of leukocytes correlated strictly with the acquisition of a polarized morphology; in one of these cases (Nieto *et al.*, 1997), moreover, the redistribution was observed for receptors other than those whose activation induced the cell polarization.

Our conclusion that receptors do not accumulate preferentially at the leading edge of migrating neutrophils should be qualified, because of the relatively low resolution of the data. Indeed, some images (e.g., Figure 8) suggest that receptor density may be very much higher on a few membrane projections at the cell's leading edge. These localized increases in receptor density may represent fixation artifact, because they were seen only in images made from fixed cells. Whether or not the increases of C5aR–GFP on membrane projections represent artifacts, we see them in cells responding to fMLP, indicating that they are not agonist specific (our unpublished result).

Possible Mechanisms for Amplifying the Chemotactic Gradient

If receptor redistribution does not amplify the chemotactic gradient, we must conclude that neutrophils use some other mechanism to detect a concentration difference as small as 1% from front to back. How might such an apparent amplification come about? At what level of the signaling pathway does amplification take place? One straightforward possibility is that increased complexity and folding of plasma membrane, which we observed at the leading edge (Figures 6 and 7), increases the sensitivity of the cell's anterior pole simply because the absolute number of receptor molecules is higher there. Tight membrane folds could also induce a significant increase in ratio of cell surface to *local* volume of cytoplasm (just beneath the membrane); an increase in this ratio would increase the intensity of the cytoplasmic signals (second messengers or activated proteins) that trigger polymerization of actin. Such mechanisms could make the cell sense an apparently steeper gradient of chemoattractant from front to back, reinforcing the cell's polarity and its persistent forward motion.

This scenario cannot be the whole story; however, as indicated by recent observations, indicating that actin-induced complex folding of plasma membrane in a pseudopod is not necessary for asymmetric detection of a chemotactic gradient by *D. discoideum* cells (Parent *et al.*, 1998). In these experiments, a cAMP gradient produced an asymmetric intracellular signal, much greater at the front than the back, even when actin polymerization was completely blocked by latrunculin, a toxin that sequesters G-actin. Assessment of the intracellular signal depended upon ligand-induced recruitment to the plasma membrane of a GFP-tagged cytoplasmic protein, the cytoplasmic regulator of adenylyl cyclase (CRAC). After latrunculin treatment, a cAMP gradient caused no apparent morphological polarity, because actin was not polymerized; in the same cells, however, the cAMP gradient caused recruitment of CRAC-GFP to surfaces of the cells facing the pipette, rather than the side away from the pipette. Thus actin-induced membrane folds may facilitate directional motility, but are probably not required for asymmetric detection of a gradient, at least in so far as neutrophils use detection mechanisms similar to those of *D. discoideum*.

If this inference applies to the chemotactic-signaling mechanisms of neutrophils and other eukaryotic cells, it will be necessary to look for other molecular mechanisms that may amplify asymmetry of the chemotactic signal. Does amplification of the signal depend upon asymmetric activity or ligand affinity of receptors, or does it take place at a downstream site, involving concentrations, recruitment, or activities of G proteins, RGS (regulators of G protein signaling) (Dohlman and Thorner, 1997; Berman and Gilman, 1998), or effector molecules? Many scenarios have been suggested (Walter and Marasco, 1987; Devreotes and Zigmond, 1988), but none so far is supported by real evidence. Answers will come from a combination of genetic analysis, real-time observations of chemotaxis in model systems like the PLB-985 cell, and biochemical dissection of the signals that link receptors and G proteins to polymerization of actin.

ACKNOWLEDGMENTS

We thank members of the Bourne laboratory for valuable discussion, and the following individuals for their gifts: A. Abo for the PLB-985 cell line; J.M. Bishop for the Ψ2 packaging cell line and the pLNCX retroviral vector; J.A. Ember and T.E. Hugli for the polyclonal anti-C5aR antibody; and C. Gerard for the C5aR cDNA. We also thank William Hyun and Jane Gordon of the Laboratory for Cell Analysis for their help with FACS. This work was supported in part by National Institutes of Health grants GM-27800 and CA-54427 (H.R.B.) and GM-25101 (J.W.S.). G.S. is a Medical Research Council of Canada Postdoctoral Fellow, and O.D.W. is a Howard Hughes Medical Institute Predoctoral Fellow.

REFERENCES

Agard, D.A., Hiraoka, Y., Shaw, P., and Sedat, J.W. (1989). Fluorescence microscopy in three dimensions. Methods Cell Biol. *30*, 353–377.

Baggiolini, M. (1998). Chemokines and leukocyte traffic. Nature *392*, 565–568.

Barak, L.S., Ferguson, S.S., Zhang, J., and Caron, M.G. (1997a). A β-arrestin/green fluorescent protein biosensor for detecting G protein-coupled receptor activation. J. Biol. Chem. *272*, 27497–27500.

Barak, L.S., Ferguson, S.S., Zhang, J., Martenson, C., Meyer, T., and Caron, M.G. (1997b). Internal trafficking and surface mobility of a functionally intact β2-adrenergic receptor-green fluorescent protein conjugate. Mol. Pharmacol. *51*, 177–184.

Berman, D.M., and Gilman, A.G. (1998). Mammalian RGS proteins: barbarians at the gate. J. Biol. Chem. *273*, 1269–1272.

Bokoch, G.M. (1995). Chemoattractant signaling and leukocyte activation. Blood *86*, 1649–1660.

Cassimeris, L., and Zigmond, S.H. (1990). Chemoattractant stimulation of polymorphonuclear leukocyte locomotion. Semin. Cell Biol. *1*, 125–134.

Dana, R., Leto, T.L., Malech, H.L., and Levy, R. (1998). Essential requirement of cytosolic phospholipase A2 for activation of the phagocyte NADPH oxidase. J. Biol. Chem. *273*, 441–445.

Davis, B.H., Walter, R.J., Pearson, C.B., Becker, E.L., and Oliver, J.M. (1982). Membrane activity and topography of F-Met-Leu-Phe-treated polymorphonuclear leukocytes. Acute and sustained responses to chemotactic peptide. Am. J. Pathol. *108*, 206–216.

Devreotes, P.N., and Zigmond, S.H. (1988). Chemotaxis in eukaryotic cells: a focus on leukocytes and *Dictyostelium*. Annu. Rev. Cell Biol. *4*, 649–686.

Dohlman, H.G., and Thorner, J. (1997). RGS proteins and signaling by heterotrimeric G proteins. J. Biol. Chem. *272*, 3871–3874.

Downey, G.P. (1994). Mechanisms of leukocyte motility and chemotaxis. Curr. Opin. Immunol. *6*, 113–124.

Drapeau, G., Brochu, S., Godin, D., Levesque, L., Rioux, F., and Marceau, F. (1993). Synthetic C5a receptor agonists. Pharmacology,

metabolism and in vivo cardiovascular and hematologic effects. Biochem. Pharmacol. *45*, 1289–1299.

Gerard, N.P., and Gerard, C. (1991). The chemotactic receptor for human C5a anaphylatoxin. Nature *349*, 614–617.

Gerisch, G., and Keller, H.U. (1981). Chemotactic reorientation of granulocytes stimulated with micropipettes containing fMet-Leu-Phe. J. Cell Sci. *52*, 1–10.

Gray, G.D., Hasslen, S.R., Ember, J.A., Carney, D.F., Herron, M.J., Erlandsen, S.L., and Nelson, R.D. (1997). Receptors for the chemoattractants C5a and IL-8 are clustered on the surface of human neutrophils. J. Histochem. Cytochem. *45*, 1461–1467.

Hiraoka, Y., Sedat, J.W., and Agard, D.A. (1990). Determination of three-dimensional imaging properties of a light microscope system. Partial confocal behavior in epifluorescence microscopy. Biophys. J. *57*, 325–333.

Hiraoka, Y., Swedlow, J.R., Paddy, M.R., Agard, D.A., and Sedat, J.W. (1991). Three-dimensional multiple-wavelength fluorescence microscopy for the structural analysis of biological phenomena. Semin. Cell Biol. *2*, 153–165.

Huey, R., and Hugli, T.E. (1985). Characterization of a C5a receptor on human polymorphonuclear leukocytes (PMN). J. Immunol. *135*, 2063–2068.

Huttenlocher, A., Palecek, S.P., Lu, Q., Zhang, W., Mellgren, R.L., Lauffenburger, D.A., Ginsberg, M.H., and Horwitz, A.F. (1997). Regulation of cell migration by the calcium-dependent protease calpain. J. Biol. Chem. *272*, 32719–32722.

Iiri, T., Homma, Y., Ohoka, Y., Robishaw, J.D., Katada, T., and Bourne, H.R. (1995). Potentiation of Gi-mediated phospholipase C activation by retinoic acid in HL-60 cells. Possible role of G gamma 2. J. Biol. Chem. *270*, 5901–5908.

Janeczek, A.H., Marasco, W.A., van Alten, P.J., and Walter, R.J. (1989). Autoradiographic analysis of formylpeptide chemoattractant binding, uptake and intracellular processing by neutrophils. J. Cell Sci. *94*, 155–168.

Johansson, B., Wymann, M.P., Holmgren-Peterson, K., and Magnusson, K.E. (1993). N-formyl peptide receptors in human neutrophils display distinct membrane distribution and lateral mobility when labeled with agonist and antagonist. J. Cell Biol. *121*, 1281–1289.

Konteatis, Z.D., Siciliano, S.J., Van Riper, G., Molineaux, C.J., Pandya, S., Fischer, P., Rosen, H., Mumford, R.A., and Springer, M.S. (1994). Development of C5a receptor antagonists. Differential loss of functional responses. J. Immunol. *153*, 4200–4205.

McKay, D.A., Kusel, J.R., and Wilkinson, P.C. (1991). Studies of chemotactic factor-induced polarity in human neutrophils. Lipid mobility, receptor distribution and the time-sequence of polarization. J. Cell Sci. *100*, 473–479.

Miller, A.D., and Rosman, G.J. (1989). Improved retroviral vectors for gene transfer and expression. Biotechniques *7*, 980–982, 984–9866, 989–990.

Morgan, E.L., Ember, J.A., Sanderson, S.D., Scholz, W., Buchner, R., Ye, R.D., and Hugli, T.E. (1993). AntiC5a receptor antibodies. Characterization of neutralizing antibodies specific for a peptide, C5aR-(9–29), derived from the predicted amino-terminal sequence of the human C5a receptor. J. Immunol. *151*, 377–388.

Neptune, E.R., and Bourne, H.R. (1997). Receptors induce chemotaxis by releasing the betagamma subunit of Gi, not by activating Gq or Gs. Proc. Natl. Acad. Sci. USA *94*, 14489–14494.

Nieto, M., Frade, J.M., Sancho, D., Mellado, M., Martinez, A.C., and Sanchez-Madrid, F. (1997). Polarization of chemokine receptors to the leading edge during lymphocyte chemotaxis. J. Exp. Med. *186*, 153–158.

Parent, C.A., Blacklock, B.J., Froehlich, W.M., Murphy, D.B., and Devreotes, P.N. (1998). G protein signaling events are activated at the leading edge of chemotactic cells. Cell *95*, 81–91.

Perez, H.D. (1994). Chemoattractant receptors. Curr. Opin. Hematol. *1*, 40–44.

Prossnitz, E.R., and Ye, R.D. (1997). The N-formyl peptide receptor: a model for the study of chemoattractant receptor structure and function. Pharmacol. Ther. *74*, 73–102.

Schmitt, M., and Bultmann, B. (1990). Fluorescent chemotactic peptides as tools to identify the f-Met-Leu-Phe receptor on human granulocytes. Biochem. Soc. Trans. *18*, 219–222.

Sengupta, P., Chou, J.H., and Bargmann, C.I. (1996). odr-10 Encodes a seven transmembrane domain olfactory receptor required for responses to the odorant diacetyl. Cell *84*, 899–909.

Sullivan, S.J., Daukas, G., and Zigmond, S.H. (1984). Asymmetric distribution of the chemotactic peptide receptor on polymorphonuclear leukocytes. J. Cell Biol. *99*, 1461–1467.

Tarasova, N.I., Stauber, R.H., Choi, J.K., Hudson, E.A., Czerwinski, G., Miller, J.L., Pavlakis, G.N., Michejda, C.J., and Wank, S.A. (1997). Visualization of G protein-coupled receptor trafficking with the aid of the green fluorescent protein. Endocytosis and recycling of cholecystokinin receptor type A. J. Biol. Chem. *272*, 14817–14824.

Tucker, K.A., Lilly, M.B., Heck, L., Jr., and Rado, T.A. (1987). Characterization of a new human diploid myeloid leukemia cell line (PLB-985) with granulocytic and monocytic differentiating capacity. Blood *70*, 372–378.

Van Epps, D.E., Simpson, S., Bender, J.G., and Chenoweth, D.E. (1990). Regulation of C5a and formyl peptide receptor expression on human polymorphonuclear leukocytes. J. Immunol. *144*, 1062–1068.

Walter, R.J., and Marasco, W.A. (1984). Localization of chemotactic peptide receptors on rabbit neutrophils. Exp. Cell Res. *154*, 613–618.

Walter, R.J., and Marasco, W.A. (1987). Direct visualization of formylpeptide receptor binding on rounded and polarized human neutrophils: cellular and receptor heterogeneity. J. Leukocyte Biol. *41*, 377–391.

Xiao, Z., Zhang, N., Murphy, D.B., and Devreotes, P.N. (1997). Dynamic distribution of chemoattractant receptors in living cells during chemotaxis and persistent stimulation. J. Cell Biol. *139*, 365–374.

Zigmond, S.H. (1974). Mechanisms of sensing chemical gradients by polymorphonuclear leukocytes. Nature *249*, 450–452.

Zigmond, S.H. (1977). Ability of polymorphonuclear leukocytes to orient in gradients of chemotactic factors. J. Cell Biol. *75*, 606–616.

Zigmond, S.H., Levitsky, H.I., and Kreel, B.J. (1981). Cell polarity: an examination of its behavioral expression and its consequences for polymorphonuclear leukocyte chemotaxis. J. Cell Biol. *89*, 585–592.